Electrochemically deposited poly(ethylene glycol)-based sol–gel thin films on stainless steel stents

Regina Okner,[ab] Abraham Jacob Domb[a] and Daniel Mandler*[b]

Received (in Montpellier, France) 28th January 2009, Accepted 31st March 2009
First published as an Advance Article on the web 6th May 2009
DOI: 10.1039/b901864f

Poly(ethylene glycol) (PEG) was modified with 3-isocyanatopropyltriethoxysilane (IPTS) to obtain PEG-disilane. This monomer was electrochemically polymerized and deposited onto a stainless steel surface to form a thin PEGylated sol–gel film. The monomer was characterized by ^{1}H-NMR and FTIR spectroscopy. The sol–gel film was characterized by absorption–reflection infrared spectroscopy (AR-FTIR), energy dispersive X-ray analysis (EDX), cyclic voltammetry (CV), profilometry, scanning electron microscopy (SEM) and potentiodynamic polarization. AR-FTIR confirmed the formation of a polymer, while the stability of the polymeric film on stainless steel in buffer phosphate was studied by scanning electron microscopy (SEM). The polymer was successfully electrodeposited onto 316L coronary stents. Its flexibility was examined by dilating the coated stents and inspecting it by SEM. The hydrophilic, smooth PEGylated sol–gel coating significantly reduced the activation and adhesion of platelets as compared with the bare stainless steel surface. This coating, which can be applied to complex geometries, such as stents, is likely to serve as an excellent biomaterial.

Introduction

The surface properties of blood-contacting materials play a crucial role in the development of biocompatible devices.[1,2] Significant efforts, aiming at surface modification to minimize biological response induced by platelet adhesion and activation, have been attempted.[3,4] A number of anti-coagulants, such as poly(ethylene glycol) (PEG),[5] poly(ethylene oxide)–poly(propylene oxide)–poly(ethylene oxide) (PEO–PPO–PEO) triblock copolymers (also called Pluronics), heparin,[6,7] and phospholipids,[8] are known for their ability to successfully reduce protein and platelet adsorption. Among them, PEG[9–11] and pluronic acid modified surfaces have shown particular effectiveness as compared with other polymers presumably due to their physical properties.[12,13] The most important characteristics of PEG are its high hydrophilicity, non-toxicity, non-immunogenicity and flexibility, the latter depending on its molecular weight. However, PEG alone lacks appropriate mechanical properties that are essential for biomedical applications, especially for thin coating. A common solution is to modify the biomaterial with PEG. Accordingly, a significant reduction of platelet adhesion was shown by modifying polyurethanes,[14,15] cellulose membranes,[16] poly-(ethylene terephthalate)[17] and self-assembled monolayers[18,19] with different PEG derivatives. Surface modification methods vary from physical adsorption, imbedding into the main polymeric matrix to covalent binding to the surface.[18,20–22]

Since stable and non-biodegradable coating is essential for blood-contact devices, covalent modification of the device coating with PEG derivatives is the most advantageous method. This can be accomplished by surface grafting with PEG chains[9,17,23–25] or by preparing PEG derived monomers[26] and further polymerization on the desirable device.

As a result, a number of strategies have been introduced for coating stainless steel, which is a representative metal for biomedical application, with PEG derivatives. These include surface silanization with epoxy precursors, followed by grafting of PEG chains,[27,28] PEG spin-coating with RF-plasma mediated crosslinking[28,29] and polyethyleneimine thin films modified with aldehyde-terminated PEG chains.[30] Furthermore, Park *et al.* introduced modified Nitinol (which is a Ni–Ti alloy) stent with PEG and Pluronic through surface silanization, followed by γ-irradiation for covalent grafting.[31]

This study describes a single-step electrodeposition of sol–gel films based on PEG modified silanes as a means of forming biocompatible and non-biodegradable coatings for metallic implants.

Sol–gel technology has been well known for more than a century[32] and its rapid development during the last twenty years has made it widely applicable in medicine and fields where thin films are sought.[33,34] Sol–gel formation proceeds through hydrolysis and condensation of mostly alkoxy metals, *e.g.*, tetramethoxysilane, that are catalyzed under acidic or basic conditions.[35] Sol–gel film methodology has been explored and developed substantially during the last decade.[36] Formation of sol–gel thin films on different surfaces can be carried out by dip- and spin-coating[33] or spraying the sol onto the substrate followed by its condensation.[35]

Electrodeposition of sol–gel films onto conducting surfaces was developed in our laboratory a decade ago.[37] The method is based on applying a negative potential to the stent which

[a] *Department of Medicinal Chemistry and Natural Products, School of Pharmacy–Faculty of Medicine, The Hebrew University of Jerusalem, Jerusalem 91120, Israel. E-mail: avid@ekmd.huji.ac.il; Fax: +972 2 5428688; Tel: +972 2 5429410*
[b] *Institute of Chemistry, The Hebrew University of Jerusalem, Jerusalem 91904, Israel. E-mail: mandler@vms.huji.ac.il; Fax: +972 2 6585319; Tel: +972 2 6585831*

causes the generation of hydroxyl ions and thus catalyzes the condensation of the sol–gel. Since then this approach has been used by others for different applications.[38–42]

Here we report the synthesis, characterization and electrodeposition of PEG silanated sol–gel onto a stainless steel surface and its application as an anti-coagulant coating on coronary stents. The two most important problems of stent implantation are restenosis and thrombosis. The major effort is directed towards reducing the occurrence of *in-stent* restenosis which is accomplished by approved DES systems (reduction in 40–60% of cases compared to bare metal stent). However, the risk of the surface-induced thrombosis formation, especially late thrombosis, still remains after DES implantation. The thrombosis, which is caused by blood protein adsorption, can be prevented by implant surface modification with hydrophilic protein antifouling molecules, such as PEGs.

Several approaches for creating hydrophilic silanated stents have already been demonstrated[43] using spraying or dipping method. The major advantage of sol–gel electrodeposition lies in the ability to selectively coat only the conducting parts of a surface and follow closely their intimate morphology. Moreover, coating is highly controlled by the applied potential and its duration. Specifically, we prepared short (M_w 200 and 400) PEG silane monomers, *i.e.*, PEG-di(*N*-triethoxysilylpropyl-carbamate (PEGdiIPTS).[18] This silane monomer was electrodeposited on the stainless steel surface and analyzed by cyclic voltammetry (CV), reflection–absorption infrared spectroscopy (AR-FTIR), contact angle, atomic force microscopy (AFM) and scanning electron microscopy (SEM). The corrosion resistance of this film in Hank's solution was also studied. Finally, we found a substantial decrease in platelet adhesion to the PEGylated silane surface as compared with a bare stainless steel stent.

Experimental

Materials

316L stainless steel plates (1 × 10 × 20 mm), disks (1 mm thickness and 14 mm diameter) and stents (length of 12 mm, a surface area of ~48 mm^2, and a closed diameter of 1.8 mm) were produced by STI Laser Industries, Israel. Poly(ethylene glycol) (PEG, M_w 200 or 400) was obtained from Fluka; 3-isocyanatopropyltriethoxysilane (IPTS; 95%), stannous octanoate ($Sn(Oct)_2$), Hank's balanced salt solution and other reagents were obtained from Sigma-Aldrich and used without further purification. Silica gel for column chromatography was purchased from Merck, Germany. All aqueous solutions were prepared from deionized water (Barnstead Easypure UV system).

Instrumentation

Electrochemical measurements were conducted with a 750B electrochemical analyzer (CH Instruments, TX) using a three-electrode cell with $Ag/AgCl_{(KCl\ sat)}$ in water medium) or Ag/AgBr (in organic medium) as a reference electrode and a Pt wire as a counter electrode. The working electrodes were of three types: 316L stainless steel plates, disks and stents.

External reflection–absorption infrared spectra (RA-FTIR) were recorded using an Equinox 55 (Bruker) spectrometer equipped with a nitrogen-cooled mercury cadmium telluride detector at a resolution of 2 cm^{-1}. *Measurement of monomers*: transmittance spectra were acquired with NaCl disks. Typically 50 scans were collected *versus* a reference. *Measurements of electrodeposited films*: the spectra were acquired with a grazing angle accessory having an incident angle of 80° to the normal and a p-polarized beam. Typically, 500 scans were collected *versus* a reference, which was a bare stainless steel surface.

Contact angles were measured with a Ramé–Hart model 100 contact angle goniometer. These measurements were repeated three times for each sample, and the average values are reported.

Thicknesses of the polymer coatings were determined by profilometry (P-15, KLA-Tencor Co., USA). Specifically, the profiles were recorded across a notch, which was manually scratched by a wooden stick before heating to 100 °C.

AFM measurements were conducted using a Nanoscope Dimension 3100 scanning probe microscope with a Nanoscope IVa controller.

Surfaces of the electrodeposited films were inspected by scanning electron microscopy (SEM) using an analytical Quanta 200 environmental scanning electron microscope (ESEM, FEI company) equipped with an EDX detector. Film coatings were sputter-coated with a very thin Au/Pd layer using a Polaron SC7640 Sputter Coater.

An impact cone and plate(let) analyzer was used for whole-blood platelet function testing. The apparatus consists of a cone and a well (plate) (see Fig. 1). A small drop of blood is placed onto the well followed by application of the cone that is rotated at a determined velocity. This unique design allows for platelet function testing under conditions that mimic the physiological flow within the human blood vessel, thus

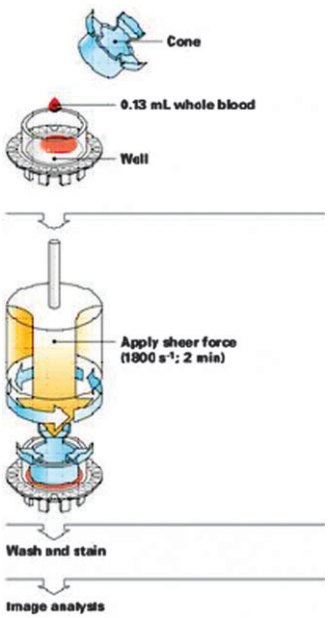

Fig. 1 Schematic presentation of cone and plate(let) analyzer procedure (reproduced with permission by Herewith Matis Medical Ltd).

achieving the most accurate and authentic pattern of platelet function. The test requires minimal blood volume and no blood processing.

Synthesis of PEG400/200di(*N*-triethoxysilylpropylcarbamate) (PEG400/200-diIPTS) (Scheme 1)

PEG400/200-diIPTS was synthesized according to a reported procedure[18,44] with minor changes. 10 g of PEG400/200 were dissolved in toluene in a three-necked round bottom flask equipped with a mechanic stirrer and dried under azeotropic reflux until no more water was observed on the bottom of the Dean Stark tube. Then, the solution was cooled down to 80 °C and $Sn(Oct)_2$ was added to the dry polymer (1 : 10 molar ratio) under a gentle flow of N_2. The mixture was stirred for 5 min and then IPTS (2.3 eq.), dissolved in dry dioxane, was added dropwise for 1 h. The mixture was stirred for an additional hour and then cooled down. The solvents were evaporated and the viscous residue was purified from free silane monomers using silica gel column chromatography with 10% MeOH in dichloromethane as an eluent. ^{1}H-NMR (300 MHz; $CDCl_3$; Me_4Si): δ 0.60 (t, $-CH_2Si$), 1.21 (t, $-OCH_2CH_3$), 1.57 (m, $-CH_2CH_2CH_2Si$), 3.15 (t, $-CH_2CH_2CH_2Si$), 3.62 (m, $-(CH_2CH_2O)_n-$), 3.84 (q, $-OCH_2CH_3$), 4.11 (t, $-CH_2OC(O)NH-$).

Hydrolysis and electrodeposition of PEG400/200-diIPTS

The solution for the electrodeposition of sol–gel films consisted of 1 mL silane monomer, 2.5 mL 0.1 M HCl and 6.5 mL ethanol. Hydrolysis was carried out by stirring this solution for 2 h at room temperature. Then, a constant negative potential of −1 V *vs.* Ag/AgBr was applied to the electrode for 1–30 min. The hydrolyzed solution was stable for more than 3 weeks. The coated electrodes were carefully withdrawn from the solution and dried for 24 h in air and then were cured at 100 °C for 18 h.

Electrochemical analysis

Cycling voltammetry (CV) of hexammineruthenium(III) chloride in 0.1 M KCl was recorded by cycling the potentials between 0 and −0.4 V *vs.* Ag/AgCl. Potentiodynamic polarization was carried out in a Hank's balanced salt solution. The scan rate was 2 mV s^{-1}.

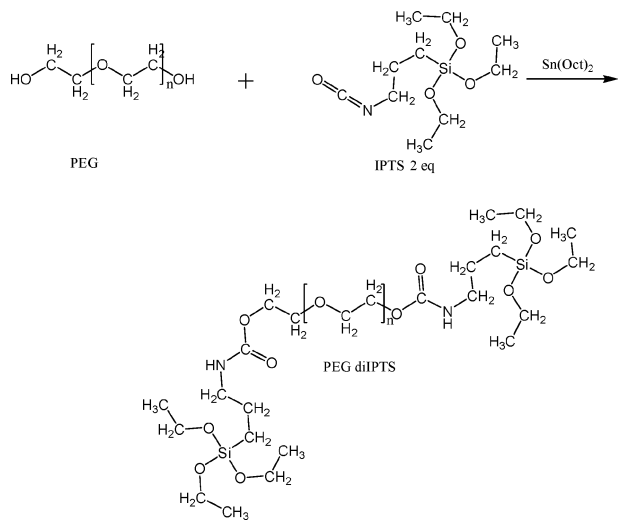

Scheme 1 Synthesis of PEG400/200-diIPTS.

Stent coating analysis

Stents were coated with PEG200/400diIPTS as described in the section 'Hydrolysis and Electrodeposition of PEG400/200-diIPTS'. The coated stents were mounted on the catheter balloon and expanded up to a final inner diameter of 3 mm, while soaking in buffer phosphate solution for 1 min. Expanded samples were kept in phosphate buffer solution (pH 7.4) for one week.

Blood compatibility evaluation

For platelet adhesion studies, stainless steel disks of 1 mm thickness and 14 mm diameter were placed into the well of a cone and plate(let) analyzer (Fig. 1) and 130 μL of the citrated fresh blood sample (40 min after withdrawing from the healthy adult) were applied to the disk. After mounting the cone, the stainless steel disk with the blood was subjected to arterial shear flow (1800 s^{-1}) for 2 min. Then, the disks were gently washed with PBS solution and adsorbed platelets were fixed by 2.5% glutaraldehyde solution for 30 min at room temperature. Finally disks were washed with PBS solution, followed by subsequent washing in 50%, 75% and 100% ethanol and dried.

Results and discussion

Nowadays stents are usually coated with a thin film to enhance their biocompatibility as well as to accommodate a drug that its release is controlled. Most of the films which are employed are indeed biocompatible; however, they do not prevent protein adsorption and platelet adhesion. We have recently[39] shown that sol–gel thin films can be electrochemically coated by applying moderate potentials, which alter the pH on the electrode surface and therefore catalyze the condensation of the hydrolyzed sol–gel precursor. There are numerous commercially available sol–gel precursors, most of them are trialkoxysilane derivatives.

We have decided to examine the electrochemical formation of a sol–gel thin film on stent, which will prevent platelet adhesion. Hence, we synthesized silanated PEGs of two different sizes, PEG200 and PEG400, by coupling 3-isocyanatopropyltriethoxysilane (IPTS) with the hydroxyl end groups of PEG through urethane bonds. In addition, we prepared the disilane derivative of Pluronic F127 (F127diIPTS). The 1 : 2 ratio of PEG or Pluronic F127 to silane was proved by analysis of ^{1}H-NMR spectra of these disilanes (see Experimental). The FTIR spectra presented in Fig. 2 show the absorption of the functional groups before and after coupling. The cyanate group, which contributes a strong vibration band at 2277 cm^{-1}, is clearly seen in the IPTS spectrum and completely disappears in the PEGdiIPTS spectrum. On the other hand, urethane C–N–H bending (1540 cm^{-1}) and carbonyl vibration (1715 cm^{-1}) appear in the products. From the PEGdiIPTS spectrum, specifically the stretching vibration of $Si–O–CH_2–$ (Fig. 2) at 1060–1090 cm^{-1}, it is evident that the disilane is unhydrolyzed.

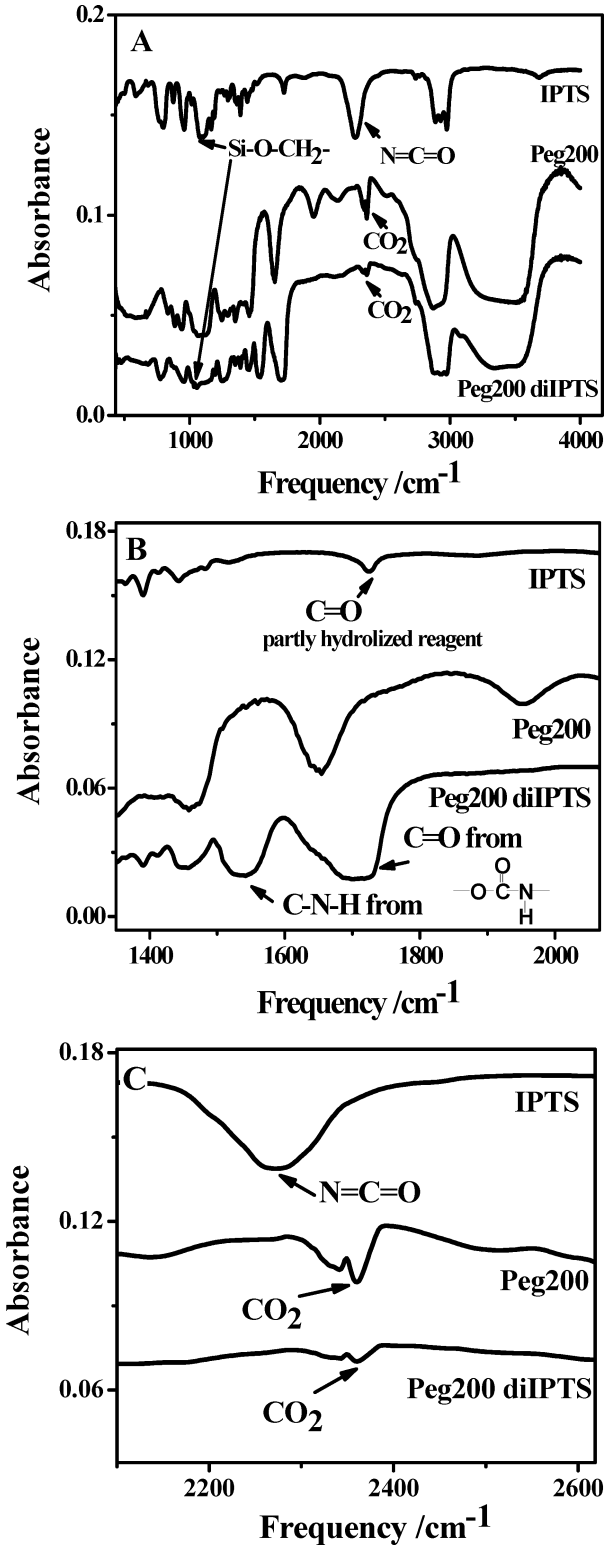

Fig. 2 FTIR spectrum of IPTS, PEG200 and PEG200diIPTS (monomer) (A). Expanded region from 1400 to 2000 cm^{-1} (B). Expanded region from 2000 to 2600 cm^{-1} (C).

PEGdiIPTSs were electrodeposited onto stainless steel plates and stents by applying a constant potential of −1 V *vs.* Ag/AgBr (*ca.* −3.5 mA cm^{-2}) for different durations ranging from 1 to 30 min. The negative potential causes the reduction of water as will be discussed below. The formation of a PEG400diIPTS-based film on a stent upon applying a potential for 15 min can be seen by scanning electron microscopy (Fig. 3).

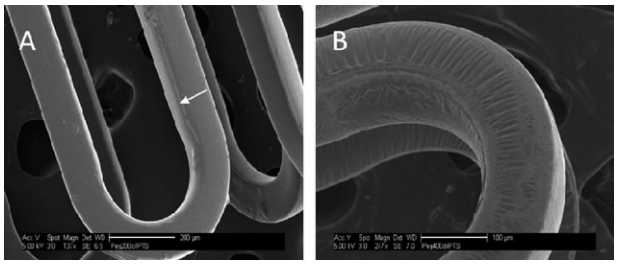

Fig. 3 SEM image of stent, coated with PEG400diIPTS. A: smooth coating; B: wrinkled site of the coating on the stent strut.

The film is usually highly uniform and smooth as shown in Fig. 3A and therefore we also purposely show an image (Fig. 3B) in which the film is somewhat wrinkled. The arrow in Fig. 3A corresponds to the edge of the stent strut, which is coated with a thinner film than the face part of the strut. This is presumably caused by the difference in the electrical field between the two electrode (stent) areas. The higher electrical field (at the edge) plus the partial radial diffusion are responsible for the massive reduction of protons and therefore the greater change of pH at these areas. The latter resulted in an intensive bubbling of hydrogen, which prevented good deposition. This phenomenon must be taken into consideration in coating medical devices, where homogeneity of the deposited film is a crucial parameter. Sol neutralization prior to the electrodeposition may help in reducing the pH leap from acidic to basic, but it caused the deposition of salt crystals on the coating surface and therefore was not preferred. Simulation of the electrical potential and field should assist in designing the proper cell which will result in the deposition of a homogenous and uniform coating.

EDX analysis (presented as At%) of coated and bare stents is shown in Table 1. The absence of iron, nickel and chromium signals pointed to the total coverage of the stent surface with sol–gel coating. Assuming full hydrolysis of the dimer yields a repetitive unit with the chemical formula $C_{26}H_{50}N_2O_{15}Si_2$ (for PEG 400 in a polymeric form). Closer inspection of the EDX analysis shows that the content of C, N and Si fits very well with the expected ratio. The content of oxygen is somewhat lower than expected for unknown reasons. Hence, EDX, which is in accordance with the NMR analysis, indicates the presence of a relatively thick polymeric film composed of a PEG400diIPTS unit.

Table 1 EDX analysis (atom%) of bare and PEG400diIPTS-coated stents

Surface element	Bare stent	PEGdiIPTS-coated stent
C	0	66.26
N	0	5.54
O	0.42	22.73
Fe	62.41	0
Ni	13.51	0
Cr	19.11	0
Si	1	5.48

The growth of the sol–gel coating depends on the time that the potential is applied (Fig. 4A). The thickness of the film grows almost linearly until it reaches 0.6 μm and then it levels off as would be expected for such a process which depends on the pH gradient that is formed on the stent surface.[45] It should be noted that the decrease in the rate of film growth is not due to the blocking of the electroactive species, *i.e.*, water, as the current does not decrease during electrolysis (Fig. 4B). A minimum of 2 min of applying the potential is required to form a continuous homogenous PEGdiIPTS film.

Electrodeposited onto stainless steel, PEGdiIPTS was characterized by RA-FTIR surface spectroscopy as shown in Fig. 5. Only the relevant part of the spectrum is shown. The appearance of a strong absorption band peaked at 1130 cm^{-1} is assigned to the asymmetric Si–O–Si stretching, which is absent in the monomer spectrum (Fig. 2). This clearly indicates the formation of the polymer through Si–OH group condensation.

The silane monomer formed by coupling Pluronic F127 and IPTS, namely, F127diIPTS, failed to polymerize, perhaps due to its final structure in the water–ethanol medium. It is well known[46] that Pluronics form 3D cylindrical structures, such as hexagonal or square domains, when their concentration is higher than the critical micelle concentration (CMC). In these micelle structures the area to volume ratio decreases, which might pose a higher barrier towards condensation of the monomers.[47–49] Previous reports showed that condensation of F127diIPST monomers in solution occurs on the third day.[50]

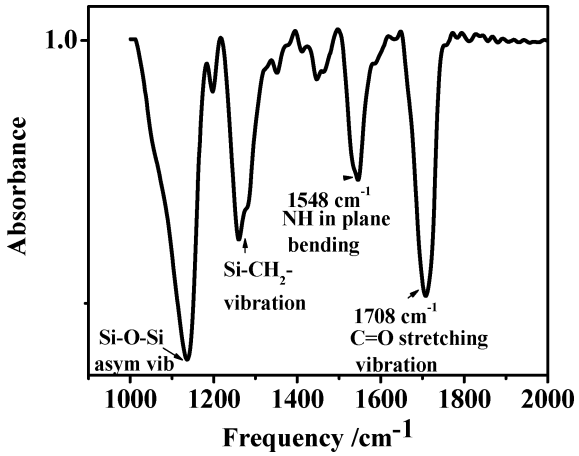

Fig. 5 RA-FTIR spectrum of PEG200diIPTS (polymer) electrodeposited on a stainless steel surface.

Sol–gel films after drying usually block electron transfer.[51] The diffusion of inorganic and organic electroactive species is strongly affected by the barrier properties of the films. Fig. 6 shows the cyclic voltammetry (CV) of bare and coated (with PEG200diIPTS) stents recorded in the presence of $Ru(NH_3)_6^{3+}$. The latter is often used as an electrochemical probe for measuring the permeability of thin films towards inorganic species.[52,53] It is evident that while the bare stent does not block electron transfer and the CV is quasi-reversible (ΔE = 215 mV), there is complete blocking of $Ru(NH_3)_6^{3+}$ reduction by the coated stent.

We found that the stability of the hydrophilic silane coating depended on thermal treatment. The thermal treatment that

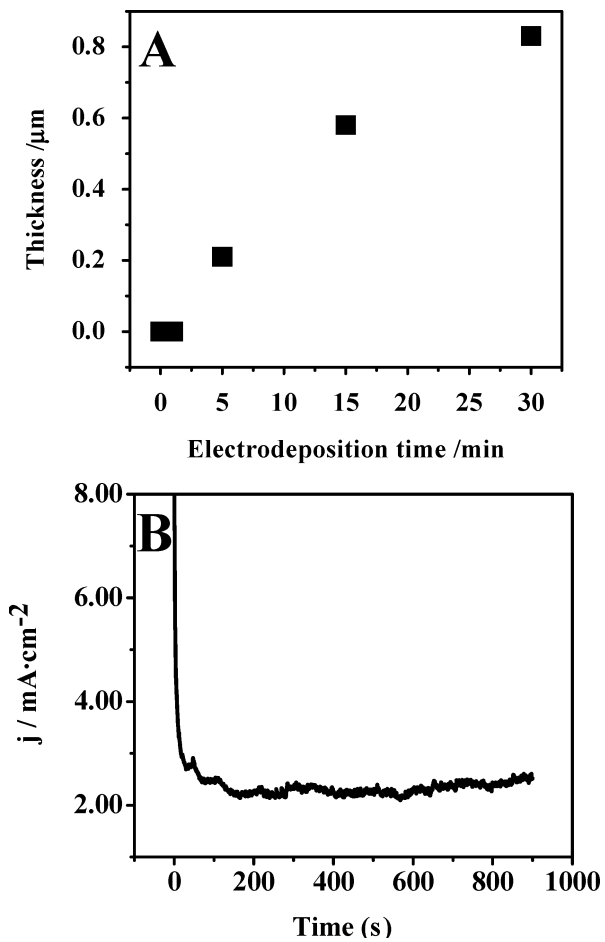

Fig. 4 (A) The thickness of a PEG400diIPTS film on a stainless steel plate as a function of the electrodeposition time (applied potential was −1 V *vs.* Ag/AgBr); (B) current transient during electrodeposition of PEG400diIPTS at constant potential.

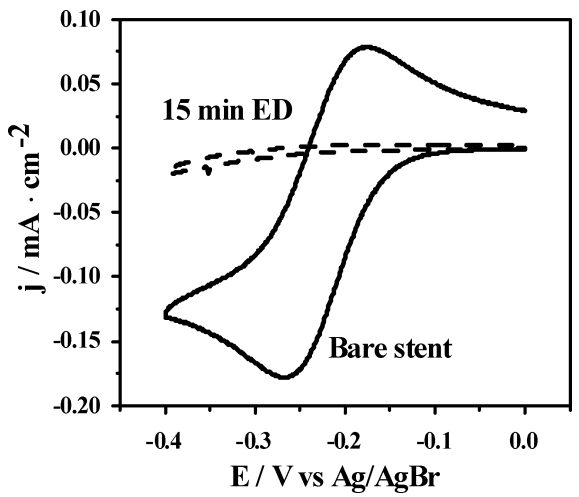

Fig. 6 Cyclic voltammetry of 1 mM $Ru(NH_2)_6^{3+}$ in 0.1 M KCl, recorded with a stainless steel stent before (continuous line) and after (dashed line) electrochemical deposition of PEG200diIPTS for 15 min at −1 V *vs.* Ag/AgBr. Scan rate equals 100 mV s^{-1}.

gave the best results comprised drying of the freshly electrodeposited coatings in air for 24 h followed by heating to 100 °C overnight. The advantage of this treatment is clearly demonstrated by recording the potentiodynamic polarization curves (Fig. 7) of bare and PEGdiIPTS-coated plates, treated in different ways.

Potentiodynamic polarization curves present the current density (on a logarithmic scale) as a function of the applied potential measured in corroding medium (here, Hank's solution). The corrosion protection of metals with sol–gel materials was well studied. Aluminium protection was achieved by electrodeposition of different organosilanes as was described by Sheffer *et al.*[54,55] Roux *et al.* suggested anticorrosion protection for iron and mild steel with polypyrrole–xerogel composites.[56] In addition, some corrosion inhibitors, such as chloranil, were incorporated into sol–gel matrices.[57] Fig. 7 shows the polarization curves of a bare stainless steel plate (A), an electrochemically deposited film without thermal treatment (B), a dip-coated film (C) and finally an electrochemically coated and treated (100 °C) film (D).

The information that can be obtained from these plots is derived from E_{corr}, which is the potential of the minimum current, the magnitude of the current density at potentials more positive than E_{corr} and from the linear part of the curve close to E_{corr} (Tafel plot). In general, a surface is more corrosion resistant when its E_{corr} is more positive. Furthermore, a more resistive surface will exhibit lower current densities at higher potentials. Finally, the exchange current density (which is the extrapolated current at E_{corr} derived from the linear curve) is expected to be lower for more corrosion resistant surfaces.

All these parameters are summarized in Table 2. It can be seen that E_{corr} of the thermally treated coatings is indeed more positive than the bare as well as the non-thermally treated coating. The current densities measured at −0.2 V also follow this trend and are significantly lower (notice that it is a logarithmic scale) for the thermally treated coating. The

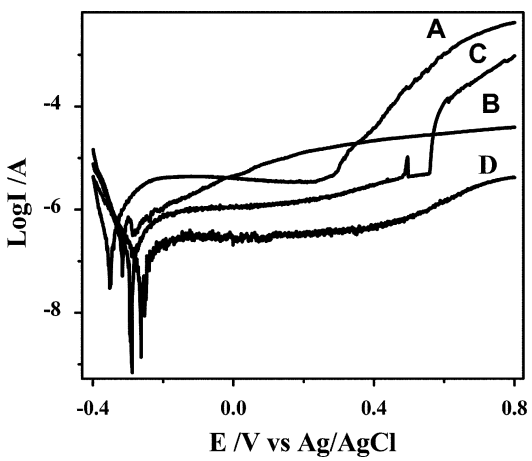

Fig. 7 Polarization curves of bare (A), electrodeposited PEG400-diIPTS (B), dip-coated with PEG400diIPTS (C) and electrodeposited PEG400diIPTS followed by thermal treatment at 100° (D) stainless steel plates. Measurements were carried out in Hank's solution with a scan rate of 2 mV s^{-1}.

Table 2 Corrosion parameters for a bare stainless steel plate (A), electrochemically deposited film without thermal treatment (B), dip-coated film with thermal treatment (C), and electrochemically coated and treated (100 °C) film (D)

	Sample			
Parameters	A	B	C	D
E_{corr} (V *vs.* Ag/AgBr)	−0.35	−0.31	−0.28	−0.26
I_{corr}/nA	30	53	2.8	1.4
Currents at −0.2 V/mA	5	1.02	0.8	0.23

current densities at more positive potentials increase substantially for the bare and non-thermally treated samples. This corresponds to pitting corrosion as is also detected by SEM, *vide infra*. It is worth mentioning that the thermally treated samples do not show such pitting corrosion at the same range of potentials implying that the coating is chemically stable under these conditions. Finally, the exchange currents, I_{corr}, which correlate with the rate of electron transfer in equilibrium and therefore are an indication of the barrier properties of the interface, show the same order (Table 2). The lower I_{corr} is found for the thermally treated electrodeposited coating, while the largest I_{corr} is for the bare plate.

In conclusion, studying the corrosion resistance of the coatings by linear polarization clearly shows the advantage of electrodeposition combined with thermal treatment.

SEM images recorded after the polarization experiment in Hank's solution, described above, complement the corrosion polarization test. Fig. 8 shows SEM images (two magnifications) of the four different samples used in the polarization test. Deep pits with an average radius of 50 μm are clearly seen in Fig. 8A, which corresponds to an uncoated plate.

The pitting corrosion of stainless steel 316L has been extensively studied statistically and experimentally by Bertocci *et al.*[58] and Williams *et al.*[59] more than two decades ago and later by Lunt *et al.*[60] Fig. 8B shows a PEGdiIPTS that is electrochemically coated but thermally untreated. It can be seen that a very thin coating remains on the surface and initial pitting is presumably detected. Fig. 8C shows a dip-coated PEGdiIPTS sample which was also thermally treated (100 °C). Enlarged image reveals delamination of the coating from the surface. Best results, as expected, were obtained for a plate that was electrocoated and thermally treated (Fig. 8D). It is evident that the coating remains smooth and homogeneous even after the corrosion test. Two important conclusions can be drawn from these observations: it seems that electrodeposition is responsible for good attachment to the stainless steel surface. This is confirmed by Fig. 8B, which shows that a thin and mostly continuous film is formed. On the other hand, the thermal treatment catalyzes the condensation of the polymer and therefore is responsible for thickening of the film as is clearly shown in Fig. 8C. Yet, this film which was not electrodeposited is poorly attached to the surface. It is the combination of electrodeposition and thermal treatment that provides thick and well adhered coatings.

So far, we have focused on the formation and characterization of uniform and adherent PEGylated sol–gel coatings that can be electrochemically deposited on stainless steel plates. Obviously, the electrochemical deposition of such films on

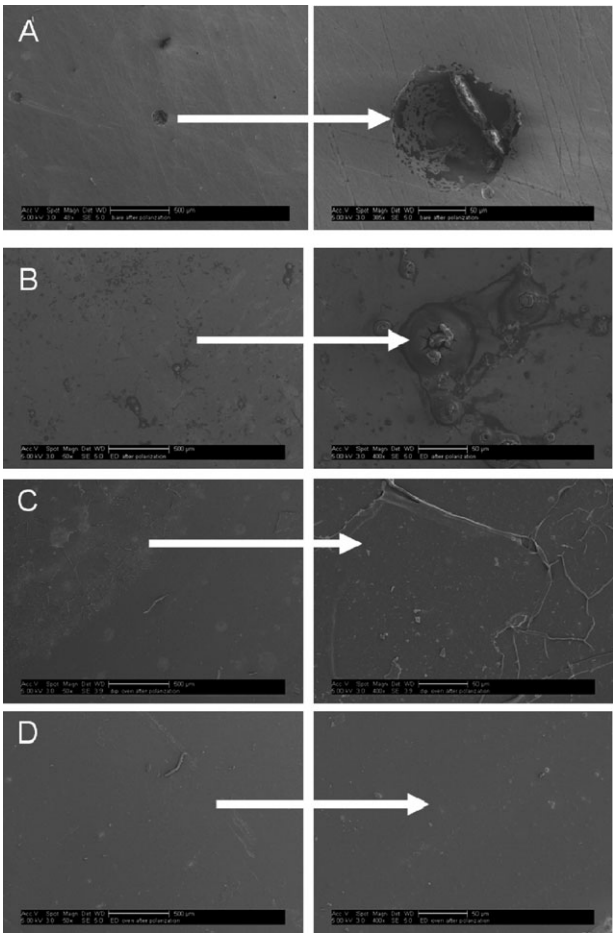

Fig. 8 SEM images (magnification of ×50 and ×400, respectively) of a bare stainless steel plate (A), an electrochemically deposited film without thermal treatment (B), a dip-coated film with thermal treatment (C) and an electrochemically coated and treated (100 °C) film (D) after the polarization experiment in Hank's solution.

stents requires some additional characteristics, such as resistance to dilatation, stability in physiological media and anti-thrombogenicity. Therefore, we conducted a few preliminary experiments whereby electrochemically and thermally treated PEGdiIPTS-coated stents were balloon expanded following a conventional procedure. Specifically, the coated stents were mounted on an expandable balloon and immersed into buffer solution for 1 minute before they were expanded from 1.8 to 30 mm inner diameter by applying a pressure of 8 atm. Coating conditions were examined after dilatation. Fig. 9 shows representative SEM images of the stent after being expanded. A low magnification image (Fig. 9A, ×34) shows stent junctions and struts covered with smooth continuous coating without any sign of cracking or delamination. Fig. 9B and C show two sites of the stent subjected to the maximal stress during expansion.

Resistance of the polymer coating to mechanical stress is one of the crucial demands of coated implantable devices. Several clinical trials revealed that surface irregularities or delaminated parts of the polymer (detected in the blood stream) are among the factors that induce fast restenosis.[61]

Fig. 9 *In situ* PEG400diIPTS-coated stent expansion. Low magnification image (×34) (A); stent sites subjected to the maximal stress during expansion (B, C). Stents were immersed into buffer phosphate solution for 1 min and then expanded from the initial diameter of 1.8 mm to a final diameter of 3 mm.

Non-biodegradable coatings of coronary stents or other implantable devices should remain intact under physiological conditions. Thus, we examined the stability of the coatings in an aqueous solution. SEM images (Fig. 10A and B) show the coated stent before and after immersing in phosphate buffer solution (pH 7.4) at 37 °C for one week. The coating remains mostly on the stent surface, indicating the strong adhesion of the sol–gel layer to the stent surface. Furthermore, this also implies that the PEG groups did not undergo hydrolysis and remain covalently attached to the sol–gel matrix.

PEG-modified composites, *vide supra*, have attracted considerable attention as cell-repelling biomaterials mostly due to their hydrophilicity and smoothness. These two parameters play a major role in designing biocompatible surfaces. Affecting platelet accumulation on coated stainless steel stents has been reported by Seeger *et al*. They showed that stainless steel stents modified with hydrophilic polymers such as *N*-vinylpyrrolidone decreased significantly platelet accumulation.[62] Park *et al*. used PEG modified Nitinol stents[31] for the same purpose. *In vitro* studies showed substantial reduction in fibrinogen adsorption and platelet adhesion to the PEG-grafted surfaces as compared with bare Nitinol surfaces. Fibrinogen adsorption was reduced by 70–95% by PEG grafting.

The contact angle of water on the PEGdiIPTS-based film was 32.1° ± 1.3°, which indicated the high hydrophilicity of the surface as compared to 60°, which was measured on the stainless steel surface. The roughness (R_q), measured on 25 × 25 μm area by AFM, was *ca*. 2.1 nm implying a very smooth coating. Hence, we examined the ability of PEGdiIPTS surfaces to reduce platelet adhesion and activation and compared these results with a pristine stainless steel surface.

For this purpose whole-blood samples were applied directly onto PEGdiIPTS coating and bare metal. The cone and

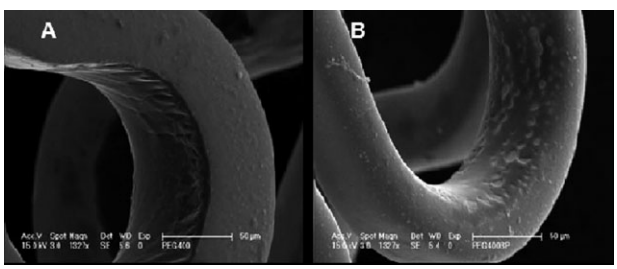

Fig. 10 SEM images of PEG400diIPTS-coated stents before (A) and after (B) immersed in phosphate buffer at 37 °C for a week.

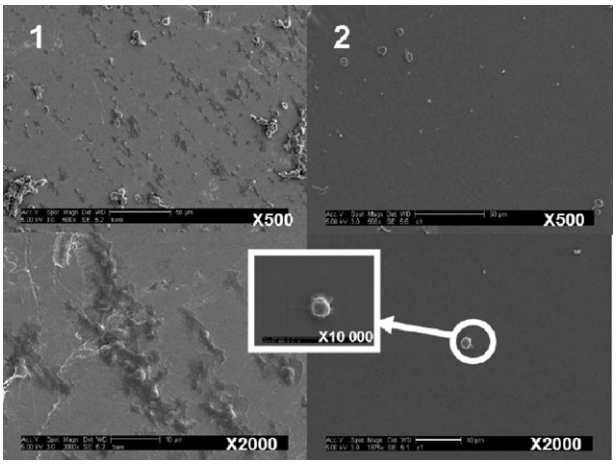

Fig. 11 SEM micrographs of platelet adhesion onto uncoated (1) and PEG400diIPTS-coated stainless steel disks (2).

plate(let) analyzer generates normal flow conditions; specifically it induces laminar flow with uniform shear force at each point of the analyzed surface. This procedure is described in detail by Varon and Savion.[63] Platelet adsorption onto bare and PEGdiIPTS-coated stainless steel surface was examined by SEM (Fig. 11). The images of the bare surface reveal numerous platelets with profuse pseudopodia. Platelets appear mostly as aggregates on the bare metal. On the other hand, the PEGdiIPTS-coated surface attracted only very few inactivated platelets. This left the surface almost unchanged. These results clearly show the advantage of PEGdiIPTS-based films as a superior coating for blood-contacting stents.

Conclusions

It is the first time, to the best of our knowledge, that PEG was electrochemically deposited under mild potentials. Short (M_w = 400; 200) poly(ethylene glycol) chains were chemically modified with trialkoxysilanes and then electrochemically polymerized on stainless steel plates and stents. PEGylated films exhibit high hydrophilicity and smoothness. The thickness of the electrodeposited coatings varied between 0.2 and 1 μm depending on the specific conditions, such as time and potential of deposition as well as silane concentration. Thermally treated PEGylated sol–gel improved significantly the corrosion protection in standard salt solutions. Electrodeposition of the PEGylated polymer on a stainless steel surface resulted in a homogeneous, stable (in buffer phosphate solution) and flexible (during balloon expansion) coating. Finally, we demonstrated that this coating is an excellent biomaterial for blood-contacting devices as it reduces dramatically adhesion and activation of platelets.

Acknowledgements

Varon *et al.* are warmly acknowledged for assisting in performing the blood platelet function test. The Harvey M. Krueger Family Center for Nanoscience and Nanotechnology of the Hebrew University is acknowledged.

References

1 G. W. Roach, M. Kanchuger, C. M. Mangano, M. Newman, N. Nussmeier, R. Wolman, A. Aggarwal, K. Marschall, S. H. Graham, C. Ley, G. Ozanne and D. T. Mangano, *New Engl. J. Med.*, 1996, **335**, 1857–1863.
2 J. M. Journeycake and G. R. Buchanan, *Curr. Opin. Hematol.*, 2003, **10**, 369–374.
3 A. S. Hoffman, *Ann. N. Y. Acad. Sci.*, 1987, **516**, 96–101.
4 C. P. Sharma, *Bull. Mater. Sci.*, 1994, **17**, 1317–1329.
5 M. Amiji and K. Park, *J. Biomater. Sci., Polym. Ed.*, 1993, **4**, 217–234.
6 O. Larm, R. Larsson and P. Olsson, *Biomater. Med. Devices, Artif. Organs*, 1983, **11**, 161–173.
7 G. Bayramoglu, M. Yilmaz, E. Batislam and M. Y. Arica, *J. Appl. Polym. Sci.*, 2008, **109**, 749–757.
8 K. Ishihara, H. Hanyuda and N. Nakabayashi, *Biomaterials*, 1995, **16**, 873–879.
9 K. Holmberg, K. Bergstrom, C. Brink, E. Osterberg, F. Tiberg and J. M. Harris, *J. Adhes. Sci. Technol.*, 1993, **7**, 503–517.
10 M. Amiji and K. Park, Surface Modification of Polymeric Biomaterials With Poly(Ethylene Oxide)—A Steric Repulsion Approach, *ACS Symp. Ser.*, 1994, **540**, 135–146.
11 J. S. Tan, D. E. Butterfield, C. L. Voycheck, K. D. Caldwell and J. T. Li, *Biomaterials*, 1993, **14**, 823–833.
12 M. Amiji and K. Park, *Biomaterials*, 1992, **13**, 682–692.
13 *Poly(ethylene glycol) Chemistry: Biotechnical and Biomedical Applications*, ed. J. M. Harris, Plenum Press, New York, 1992.
14 Y. G. Wu, F. I. Simonovsky, B. D. Ratner and T. A. Horbett, *J. Biomed. Mater. Res., Part A*, 2005, **74**, 722–738.
15 H. D. Park, J. W. Bae, K. D. Park, T. Ooya, N. Yui, J. H. Jang, D. K. Han and J. W. Shin, *Macromol. Res.*, 2006, **14**, 73–80.
16 N. Tsunoda, K. Kokubo, K. Sakai, M. Fukuda, M. Miyazaki and T. Hiyoshi, *ASAIO J.*, 1999, **45**, 418–423.
17 D. S. Kumar, M. Fujioka, K. Asano, A. Shoji, A. Jayakrishnan and Y. Yoshida, *J. Mater. Sci.: Mater. Med.*, 2007, **18**, 1831–1835.
18 S. Jo and K. Park, *Biomaterials*, 2000, **21**, 605–616.
19 K. L. Prime and G. M. Whitesides, *J. Am. Chem. Soc.*, 1993, **115**, 10714–10721.
20 W. R. Gombotz, W. Guanghui, T. A. Horbett and A. S. Hoffman, *J. Biomed. Mater. Res.*, 1991, **25**, 1547–1562.
21 N. L. Burns, J. M. Vanalstine and J. M. Harris, *Langmuir*, 1995, **11**, 2768–2776.
22 J. H. Lee, H. B. Lee and J. D. Andrade, *Prog. Polym. Sci.*, 1995, **20**, 1043–1079.
23 B. Balakrishnan, D. S. Kumar, Y. Yoshida and A. Jayakrishnan, *Biomaterials*, 2005, **26**, 3495–3502.
24 E. Uchida, Y. Uyama and Y. Ikada, *Langmuir*, 1994, **10**, 481–485.
25 O. Iguerb and P. Bertrand, *Surf. Interface Anal.*, 2008, **40**, 386–390.
26 J. F. Lutz, *J. Polym. Sci., Part A: Polym. Chem.*, 2008, **46**, 3459–3470.
27 C. K. Kang and Y. S. Lee, *J. Mater. Sci.: Mater. Med.*, 2007, **18**, 1389–1398.
28 F. Zhang, E. T. Kang, K. G. Neoh, P. Wang and K. L. Tan, *Biomaterials*, 2001, **22**, 1541–1548.
29 Y. Wang, E. B. Somers, S. Manolache, F. S. Denes and A. C. L. Wong, *J. Food Sci.*, 2003, **68**, 2772–2779.
30 J. Wei, D. B. Ravn, L. Gram and P. Kingshott, *Colloids Surf., B: Biointerfaces*, 2003, **32**, 275–291.
31 K. Park, H. S. Shim, M. K. Dewanjee and N. L. Eigler, *J. Biomater. Sci., Polym. Ed.*, 2000, **11**, 1121–1134.
32 M. Ebelman, *Ann. Chim. Phys.*, 1846, **16**, 129.
33 C. J. Brinker, A. J. Hurd, G. C. Frye, K. J. Ward and C. S. Ashley, *J. Non-Cryst. Solids*, 1990, **121**, 294–302.
34 D. Avnir, *Acc. Chem. Res.*, 1995, **28**, 328–334.
35 C. J. Brinker and G. W. Scherer, in *Sol-Gel Science*, Academic Press INC, San Diego, CA, 1990, ch 3.
36 Y. F. Lu, R. Ganguli, C. A. Drewien, M. T. Anderson, C. J. Brinker, W. L. Gong, Y. X. Guo, H. Soyez, B. Dunn, M. H. Huang and J. I. Zink, *Nature*, 1997, **389**, 364–368.
37 R. Shacham, D. Avnir and D. Mandler, *Adv. Mater.*, 1999, **11**, 384–388.
38 A. Walcarius, *Chem. Mater.*, 2001, **13**, 3351–3372.
39 R. Toledano, R. Shacham, D. Avnir and D. Mandler, *Chem. Mater.*, 2008, **20**, 4276–4283.

40 S. Chaterji, I. K. Kwon and K. Park, *Prog. Polym. Sci.*, 2007, **32**, 1083–1122.
41 T. M. Harrell, B. Hosticka, M. E. Power, L. Cemke, R. Hull and P. M. Norris, *J. Sol-Gel Sci. Technol.*, 2004, **31**, 349–352.
42 X. L. Luo, J. J. Xu, Y. Du and H. Y. Chen, *Anal. Biochem.*, 2004, **334**, 284–289.
43 *US Pat.*, 0 236 399, 2004.
44 H. Kim, C. Lim and S. I. Hong, *J. Sol-Gel Sci. Technol.*, 2005, **36**, 213–221.
45 K. L. Prime and G. M. Whitesides, *J. Am. Chem. Soc.*, 1993, **115**, 10714–10721.
46 J. J. Escobar-Chavez, M. Lopez-Cervantes, A. Naik, Y. N. Kalia, D. Quintanar-Guerrero and A. Ganem-Quintanar, *J. Pharm. Pharm. Sci.*, 2006, **9**, 339–358.
47 I. R. Schmolka, *Ann. N. Y. Acad. Sci.*, 1994, **720**, 92–97.
48 M. Guzman, M. R. Aberturas, F. Garcia and J. Molpeceres, *Drug Dev. Ind. Pharm.*, 1994, **20**, 2041–2048.
49 D. Attwood, J. H. Collett and C. J. Tait, *Int. J. Pharm.*, 1985, **26**, 25–33.
50 A. Sosnik and D. Cohn, *Biomaterials*, 2004, **25**, 2851–2858.
51 G. Shustak, S. Marx, I. Turyan and D. Mandler, *Electroanalysis*, 2003, **15**, 398–408.
52 A. Demoz and D. J. Harrison, *Langmuir*, 1993, **9**, 1046–1050.
53 J. Li and A. E. Kaifer, *Langmuir*, 1993, **9**, 591–596.
54 M. Sheffer, A. Groysman and D. Mandler, *Corros. Sci.*, 2003, **45**, 2893–2904.
55 M. Sheffer, A. Groysman, D. Starosvetsky, N. Savchenko and D. Mandler, *Corros. Sci.*, 2004, **46**, 2975–2985.
56 S. Roux, P. Audebert, J. Pagetti and M. Roche, *J. Mater. Chem.*, 2001, **11**, 3360–3366.
57 M. Quinet, B. Neveu, V. Moutarlier, P. Audebert and L. Ricq, *Prog. Org. Coat.*, 2007, **58**, 46–53.
58 U. Bertocci, M. Koike, S. Leigh, F. Qiu and G. Yang, *J. Electrochem. Soc.*, 1986, **133**, 1782–1786.
59 (*a*) D. E. Williams, C. Westcott and M. Fleischmann, *J. Electrochem. Soc.*, 1985, **132**, 1796–1804; (*b*) D. E. Williams, C. Westcott and M. Fleischmann, *J. Electrochem. Soc.*, 1985, **132**, 1804–1811.
60 T. T. Lunt, S. T. Pride, J. R. Scully, J. L. Hudson and A. S. Mikhailov, *J. Electrochem. Soc.*, 1997, **144**, 1620–1629.
61 R. Virmani, F. Liistro, G. Stankovic, C. Di Mario, M. Montorfano, A. Farb, F. D. Kolodgie and A. Colombo, *Circulation*, 2002, **106**, 2649–2651.
62 J. M. Seeger, M. D. Ingegno, E. Bigatan, N. Klingman, D. Amery, C. Widenhouse and E. P. Goldberg, *J. Vasc. Surg.*, 1995, **22**, 327–336.
63 N. Savion and D. Varon, *Pathophysiol. Haemostasis Thromb.*, 2006, **35**, 83–88.

